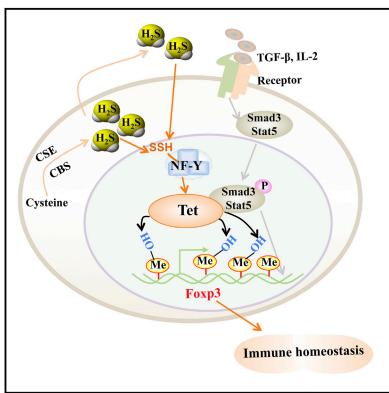# Hydrogen Sulfide Promotes Tet1- and Tet2-Mediated *Foxp3* Demethylation to Drive Regulatory T Cell Differentiation and Maintain Immune Homeostasis

Graphical Abstract

Authors

Ruili Yang, Cunye Qu, Yu Zhou, ...,
Wanjun Chen, Yanheng Zhou, Songtao
Shi

Correspondence

yanhengzhou@gmail.com (Y.Z.),
songtaos@dental.upenn.edu (S.S.)

In Brief

DNA demethylation contributes to regulation of the *Foxp3* locus but the underlying mechanism is unclear. Shi and colleagues find that hydrogen sulfide promotes expression of the methylcytosine dioxygenases Tet1 and Tet2 that mediate Foxp3 demethylation downstream of TGF-β and IL-2 signaling to promote Treg cell function and immune homeostasis.

Highlights

- H$_2$S is required for Treg cell differentiation and immune homeostasis

- H$_2$S deficiency results in decreased Tet1 and Tet2 expression in T cells

- Synergism between Tet and TGF-β and IL-2 signaling regulate Treg cell function

- Depletion of *Tet1* and *Tet2* leads to impairment of Treg cell differentiation

CrossMark

CellPress

Article

Hydrogen Sulfide Promotes Tet1- and Tet2-Mediated *Foxp3* Demethylation to Drive Regulatory T Cell Differentiation and Maintain Immune Homeostasis

Ruili Yang,[1,2,3] Cunye Qu,[3] Yu Zhou,[4] Joanne E. Konkel,[5] Shihong Shi,[3] Yi Liu,[6] Chider Chen,[2,3] Shiyu Liu,[3] Dawei Liu,[1] Yibu Chen,[7] Ebrahim Zandi,[4] Wanjun Chen,[5] Yanheng Zhou,[1,*] and Songtao Shi[2,3,*]

[1]Department of Orthodontics, Peking University School & Hospital of Stomatology, #22 Zhongguancun South Avenue, Beijing 100081, China
[2]Department of Anatomy and Cell Biology, University of Pennsylvania, School of Dental Medicine, 240 South 40th Street, Philadelphia, PA 19104, USA
[3]Center for Craniofacial Molecular Biology, Ostrow School of Dentistry, University of Southern California, 2250 Alcazar Street, CSA 103, Los Angeles, CA 90033, USA
[4]Department of Molecular Microbiology and Immunology, University of Southern California, 2011 Zonal Avenue, Los Angeles, CA 90033, USA
[5]National Institute of Dental and Craniofacial Research, NIH, 30 Convent Drive, MSC 4352 Bethesda, MD 20892, USA
[6]Laboratory of Tissue Regeneration and Immunology and Department of Periodontics, Capital Medical University School of Stomatology, #4 Tiantanxili Avenue, Beijing 100050, China
[7]Norris Medical Library, Keck School of Medicine, University of Southern California, 2003 Zonal Avenue, Los Angeles, CA 90033, USA
*Correspondence: yanhengzhou@gmail.com (Y.Z.), songtaos@dental.upenn.edu (S.S.)
http://dx.doi.org/10.1016/j.immuni.2015.07.017

SUMMARY

Regulatory T (Treg) cells are essential for maintenance of immune homeostasis. Here we found that hydrogen sulfide (H_2S) was required for Foxp3+ Treg cell differentiation and function and that H_2S deficiency led to systemic autoimmune disease. H_2S maintained expression of methylcytosine dioxygenases Tet1 and Tet2 by sulfhydrating nuclear transcription factor Y subunit beta (NFYB) to facilitate its binding to *Tet1* and *Tet2* promoters. Transforming growth factor-β (TGF-β)-activated Smad3 and interleukin-2 (IL-2)-activated Stat5 facilitated Tet1 and Tet2 binding to *Foxp3*. Tet1 and Tet2 catalyzed conversion of 5-methylcytosine (5mC) to 5-hydroxymethylcytosine (5hmC) in *Foxp3* to establish a Treg-cell-specific hypomethylation pattern and stable Foxp3 expression. Consequently, *Tet1* and *Tet2* deletion led to *Foxp3* hypermethylation, impaired Treg cell differentiation and function, and autoimmune disease. Thus, H_2S promotes Tet1 and Tet2 expression, which are recruited to *Foxp3* by TGF-β and IL-2 signaling to maintain *Foxp3* demethylation and Treg-cell-associated immune homeostasis.
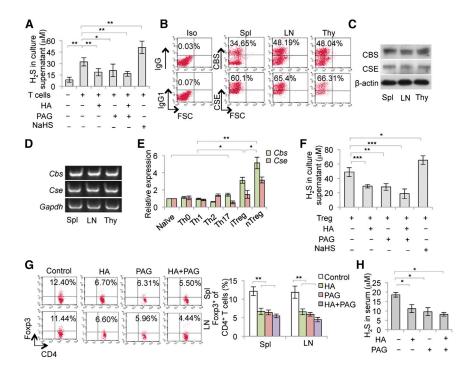
INTRODUCTION

Regulatory T (Treg) cells are a distinct lineage of CD4+ T cells that are indispensable in maintaining immune homeostasis and suppressing inflammatory reactions (Vignali et al., 2008). The forkhead-family transcription factor Foxp3 is specifically expressed in Treg cells and plays a crucial role in Treg cell lineage specification and function (Hori et al., 2003). Foxp3 deficiency results in fatal autoimmune disorders in both mice and humans (She-

vach, 2000). Treg cell development, differentiation, and function are governed by multiple epigenetic regulation mechanisms, such as DNA methylation, histone modifications, and particularly DNA demethylation of *Foxp3* promoter and conserved non-coding DNA sequence (CNS) elements (Kim and Leonard, 2007; Zheng et al., 2010). However, it remains unknown how cell signaling and epigenetic modification are synergistically coordinated to determine Treg cell lineage differentiation and achieve cell identity. DNA methylation has a profound impact on genome stability, gene transcription, and molecular and cellular responses. Recent studies indicate that the Ten eleven translocation (Tet) family is capable of converting 5-methylcytosine (5mC) to 5-hydroxymethylcytosine (5hmC) to erase existing methylation marks (Kohli and Zhang, 2013), which serve as an important epigenetics regulation mechanism (Koh et al., 2011; Song et al., 2013). However, the roles of Tet and 5hmC in immune systems, especially in Treg cell development, differentiation, and function, are unknown.

Hydrogen sulfide (H_2S), an endogenous gasotransmitter, is capable of regulating various endogenous signaling pathways. In mammals, H_2S is mainly generated by two pyridoxal-5′-phosphate-dependent enzymes, termed cystathionine β-synthase (CBS) and cystathionine γ-lyase (CSE) (Wang, 2002). Impaired H_2S metabolism might be associated with immune disorders, cancer, and hypertension (Peng et al., 2014; Szabo et al., 2013). H_2S might accentuate the inflammatory process in burn-injury-induced inflammation and lung injury caused by bacterial sepsis (Li et al., 2005; Zhang et al., 2010). On the other hand, providing H_2S through its donor might be beneficial in the treatment of colitis (Fiorucci et al., 2007), asthma (Zhang et al., 2013), and systemic lupus erythematosus (SLE) (Han et al., 2013). One of the mechanisms by which H_2S regulates inflammation is by sulfhydrating reactive Cys residues in target proteins to increase their catalytic activity (Paul and Snyder, 2012). However, the role of H_2S in inflammation is still under debate and the molecular mechanisms of H_2S in immune regulation remain largely unknown.

Figure 1. H₂S-Deficient T Cells Show Impaired Treg Cell Differentiation

(A) H_2S production in $CD4^+$ T cell culture supernatant after treatment with CBS inhibitor HA, CSE inhibitor PAG, HA and PAG combination, or H_2S donor NaHS.

(B–D) CBS and CSE expression in $CD4^+$ T cells from mouse spleen (Spl), lymph nodes (LN), and thymus (Thy) are analyzed by flow cytometry (B), immunoblot (C), and PCR (D).

(E) *Cbs* and *Cse* expression in different T cells subsets including naive, Th0, Th1, Th2, Th17, and Treg cells (iTreg and nTreg) are shown, as assessed by qPCR analysis.

(F) H_2S production in Treg cell culture supernatant in indicated groups.

(G) The frequency of Treg cells in spleen and lymph nodes after 5 weeks of HA (n = 4), PAG (n = 4), or HA and PAG combined (n = 4) treatment in mice are shown, as assessed by flow cytometry.

(H) The mouse serum concentrations after HA, PAG, or HA and PAG combined injection are shown.

Statistical significance is determined with one-way ANOVA (A, F–H). *$p < 0.05$, **$p < 0.01$, ***$p < 0.001$, (mean ± SD). Results are from three repeated experiments.

In this study, we show that Tet-mediated demethylation of *Foxp3*, in conjunction with signaling modulation, dynamically controls Treg cell lineage determination. H_2S deficiency results in reduced Tet1 and Tet2 expression, which leads to hypermethylation of *Foxp3* and, eventually, impairment of Treg cell differentiation and function and immune homeostasis.

RESULTS

Treg Cells Express CBS and CSE and Produce H₂S

Abnormal H_2S metabolism has been linked to defects in immune homeostasis, and we revealed that $CD4^+$ T cells produced H_2S in culture supernatant and that the production was downregulated by treatment with CBS inhibitor hydroxylamine (HA) or CSE inhibitor D, L-propargylglycine (PAG); conversely, H_2S concentration was upregulated by treatment with H_2S donor NaHS. Combined treatment with HA and PAG showed similar H_2S decrease as observed in the groups that received HA or PAG individually (Figure 1A). $CD4^+$ T cells from spleen, lymph nodes, and thymus of WT mice expressed both mRNA and protein of CBS and CSE (Figures 1B–1D). Expression of *Cbs* and *Cse* in Treg cells were elevated compared to other $CD4^+$ T cell subsets (Figure 1E). Treg cells also produced H_2S in the culture supernatant, which was regulated by H_2S inhibitor HA and PAG or H_2S donor (Figure 1F).

H₂S-Deficient Mice Show Treg Cell Deficiency and Autoimmune Disease

Treatment with the H_2S inhibitors HA and PAG led to reduced Treg cell numbers in mouse spleen and lymph nodes with a similar reduction observed with combined or single HA and PAG treatment (Figures 1G, 1H, and S1A). Moreover, HA, PAG, or HA and PAG treatment reduced Treg cell differentiation in vitro when cultured with different doses of TGF-β1 (Figure S1B; Chen et al., 2003).

To further examine whether H_2S serves as a physiologic gasotransmitter for regulating T cells, we analyzed Treg cell differentiation and function in H_2S-deficient ($Cbs^{-/-}$) mice (Figures S2A and S2B; Watanabe et al., 1995). $Cbs^{-/-}$ mouse serum showed decreased concentrations of H_2S compared to control ones (Figure S2C). $CD4^+$ T cells from $Cbs^{-/-}$ mice also produced less H_2S when cultured in vitro (Figure S2D). Consistent with H_2S inhibitor HA and PAG treatment, the proportion of $Foxp3^+$ Treg cells were reduced in the spleen and lymph nodes of $Cbs^{-/-}$ mice compared to control littermates (Figure 2A). The total number of Treg cells was also diminished in $Cbs^{-/-}$ mice (Figure 2B). $Cbs^{-/-}$ T cells showed compromised in vitro Treg cell differentiation when cultured with different doses of TGF-β1 (Figure 2C). Moreover, $CD4^+Foxp3^+$ Treg cells from $Cbs^{-/-}$ mice exhibited a reduced capacity to suppress $CD4^+CD25^-$ T cells, as assessed by an in vitro coculture assay (Figure 2D). To validate these findings, we generated $Cbs^{-/-}Foxp3^{GFP}$ mice by crossing $Cbs^{+/-}$ mice with $Foxp3^{GFP}$ mice. As expected, $Cbs^{-/-}Foxp3^{GFP}$ mice showed reduced numbers of GFP-labeled Treg cells compared to $Foxp3^{GFP}$ mice (Figure 2E). Moreover, Foxp3 expression was reduced in $Cbs^{-/-}$ Treg cells, as indicated by reduced mean fluorescence intensity (MFI) (Figure 2F). We observed that autoreactive antibodies, including total immunoglobulin M (IgM) (Figure 2G), anti-nuclear antibody (ANA) (Figure 2H), and anti-double strand DNA (dsDNA) IgG and IgM antibodies (Figure 2I), were more abundant in serum from $Cbs^{-/-}$ mice compared to control ones. $Cbs^{-/-}$ mice were born in expected Mendelian ratios and appeared grossly normal at the newborn stage. However, they started to lose body weight at 4 weeks of age and had a high incidence of death that might be due to inflammation of multiple organs, including the colon, lung, and liver (Figures 2J–2L and S2E). We found a consistent decrease in the proportion of Treg cells in the lung, gut, and liver of $Cbs^{-/-}$ mice (Figure S2F). Analysis of peripheral $CD4^+$ T cells
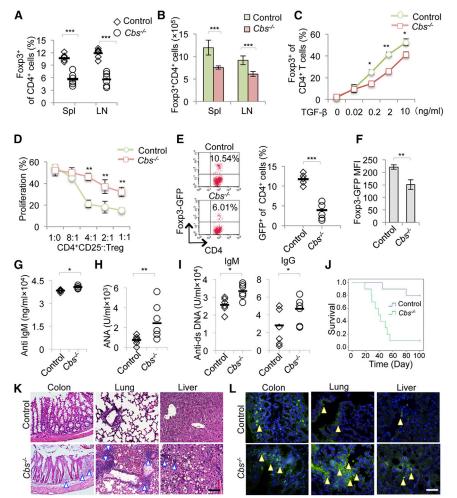
Figure 2. H₂S-Deficient Mice Show Treg Cell Impairment and Autoimmune Diseases

(A) Treg cell frequency in control and $Cbs^{-/-}$ mice spleen (Spl) and lymph nodes (LN) are assessed by flow cytometry.

(B) The total numbers of Foxp3⁺ Treg cells in control and $Cbs^{-/-}$ mice.

(C) Control and $Cbs^{-/-}$ naïve T cells in vitro differentiation induced by 2 ng/ml IL-2 and a range of doses of TGF-β are shown.

(D) Suppressive assay of Treg cells from control and $Cbs^{-/-}$ mice.

(E and F) Treg cell frequency (E) and Foxp3 (F) expression in spleen of $Foxp3^{GFP}$ and $Cbs^{-/-}$ $Foxp3^{GFP}$ mice are assessed by flow cytometry.

(G–I) Auto-reactive antibodies including anti-autoactive antibody IgM (G), anti-nuclear antibody (ANA) (H), and dsDNA antibodies IgM and IgG (I) in control and $Cbs^{-/-}$ mouse serum are measured by ELISA (n = 6).

(J) Kaplan-Meier survival curves of $Cbs^{-/-}$ mice (n = 10) and control littermates (n = 10).

(K) Histological structures of the mouse colon, lung, and liver at 5–6 weeks are shown, as assessed by hematoxylin and eosin (HE) staining. Inflammation cells infiltration is indicated (blue triangle).

(L) CD3⁺ lymphocyte infiltration (yellow triangle) in colon, lung, and liver is analyzed by immunofluorescence staining.

Statistical significance is determined by two-tailed Student's t tests (A–I), Kaplan-Meier survival curves are constructed and analyzed by a log-rank test (J, p < 0.001); *p < 0.05, **p < 0.01, ***p < 0.001 (mean ± SD). Scale bars represent HE, 100 μm. Immunofluorescence staining, 50 μm. Results are from three repeated experiments.

obtained from peripheral lymphoid organs showed that effector T cell numbers were elevated in $Cbs^{-/-}$ mice (Figure S2G). $Cbs^{-/-}$ mice showed increased numbers of CD4⁺IL-17⁺ and CD4⁺IFN-γ⁺ cells in the peripheral lymphoid organs compared to control ones, though there was no difference in the number of IL-4⁺ cells (Figures S2H and S2I), whereas CD4⁺ cell distributions in the peripheral lymphoid organs of $Cbs^{-/-}$ mice were similar to the control group (Figure S2J). To verify the role of H₂S in Treg cell development, we generated mixed bone marrow chimeras by injecting C57BL/6 (CD45.1⁺) control bone marrow with $Cbs^{-/-}$ (CD45.2⁺) bone marrow into sublethally irradiated WT recipient mice. We showed that the recipient mice had a reduced proportion of CD4⁺Foxp3⁺ Treg cells originating from $Cbs^{-/-}$ bone marrow compared to those originating from control mice (Figure S2K), indicating that endogenous H₂S production plays an essential role in Treg cell generation. To examine whether inflammation in $Cbs^{-/-}$ mice is an autoimmune response, we transferred CD4⁺ naïve T cells, derived from control and $Cbs^{-/-}$ mice, into $Rag1^{-/-}$ mice and found that $Cbs^{-/-}$ T cells elicited a more severe immune response, as indicated by signs of severe colitis and more body weight loss compared to the control group (Figures S2L–S2O). Co-transferring $Cbs^{-/-}$ Treg cells failed to prevent development of colitis in $Rag1^{-/-}$ mice, confirming the compromised suppressive capacity of

$Cbs^{-/-}$ Treg cells (Figures S2L–S2O). These data suggest that H₂S deficiency is associated with the development of autoimmune disease.

H₂S Promotes Immune Homeostasis via Regulating Treg Cells

To further determine whether Treg cell deficiency accounted for autoimmunity in $Cbs^{-/-}$ mice, we transferred WT Treg cells into $Cbs^{-/-}$ mice and found that Treg cell transfer increased body weight of $Cbs^{-/-}$ mice (Figure 3A). The elevated levels of autoreactive antibodies including anti-IgM, ANA, and anti-ds DNA antibodies in $Cbs^{-/-}$ mice were partially blocked by Treg cell transfer (Figures 3B–3D). Moreover, survival analysis indicated that WT Treg cell transfer (n = 6) extended lifespan of $Cbs^{-/-}$ mice (n = 10) (Figure 3E). The elevated inflammatory cell infiltration observed in the colon, liver, and lung of $Cbs^{-/-}$ mice was also rescued by Treg cell infusion (Figure 3F). These results indicate that Treg cell deficiency at least partially accounts for the autoimmunity developed in $Cbs^{-/-}$ mice. Microarray and gene set enrichment analysis (GSEA) of CD4⁺ T cells from $Cbs^{-/-}$ and control mice (Figures S3A and S3B) showed reduced expression of *Foxp3*-related genes in $Cbs^{-/-}$ mice (Figure S3B). The downregulated expression of *Foxp3*-related genes in CD4⁺ T cells by qPCR validated the microarray data. Moreover, the
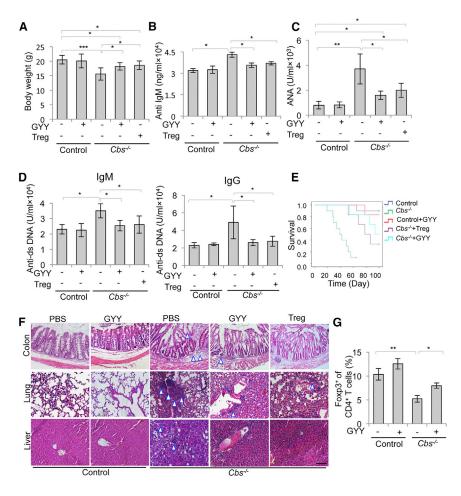
Analysis of AnnexinV, 7AAD, and Ki67 showed that the rate of apoptosis and proliferation in CD4⁺Foxp3⁺ Treg cells from $Cbs^{-/-}$ and control mice were similar (Figures S3G and S3H).

H₂S Targets Tet1 and Tet2 to Regulate Hydroxylation of 5mC

Because $Cbs^{-/-}$ Treg cells had decreased expression of Foxp3 and its target genes, including CD25, GITR, and CTLA-4 (Figure S4A), we used qPCR and immunoblot analysis to confirm that $Cbs^{-/-}$ Treg cells had decreased expression of Foxp3 (Figures 4A and S4B). We next examined why H₂S-deficient Treg cells express reduced amount of Foxp3 and found that $Cbs^{-/-}$ T cells expressed similar levels of phosphorylated Smad3 and Stat5 to those of control cells treated by TGF-β1 or IL-2 in vitro (Figures S4C and S4D), which indicates that H₂S-regulated Foxp3 expression in Treg cells might not be due to altered response to TGF-β and IL-2 signaling. Foxp3 expression is controlled by its promoter region and intragenic enhancer elements CNS1–3 (Zheng et al., 2010). CpG motifs in CNS2 are demethylated in Treg cells, which are known to be required for stable Foxp3 expression (Floess et al., 2007). Therefore, we examined the methylation status of the promoter and CNS2 in Foxp3 locus. CD4⁺CD25⁺ Treg cells and CD4⁺CD25⁻ T conventional (Tconv) cells were isolated and their methylation status was analyzed (Kim and Leonard, 2007). In comparison to Treg cells, Tconv cells showed high amounts of methylation in the promoter and CNS2 of Foxp3 locus. However, Treg cells from $Cbs^{-/-}$ mice displayed elevated methylation in the promoter and CNS2 of Foxp3 locus compared to Treg cells from control mice (Figure 4B), suggesting that H₂S plays a functional role in DNA demethylation of Foxp3 locus. Genomic DNA is mainly methylated by DNA methyltransferases (Dnmt family members), although it can be demethylated in

expression of Foxp3-related genes was downregulated in $Cbs^{-/-}$ Treg cells (Figure S3C; Zheng et al., 2007), suggesting that H₂S deficiency might affect expression of Foxp3 and its downstream genes.

We next examined whether H₂S donor treatment could rescue Treg cell numbers and autoimmunity phenotypes in $Cbs^{-/-}$ mice and showed that injection of H₂S donor GYY4137 (Figure S3D) resulted in increased serum H₂S concentrations and body weight (Figures 3A and S3E). The elevated autoreactive antibodies in $Cbs^{-/-}$ mice were partially decreased after H₂S donor treatment along with an extended lifespan and decreased inflammatory cell infiltration in the colon, liver, and lung of $Cbs^{-/-}$ mice (Figures 3B–3F). The frequency of Treg cells was elevated by GYY4137 treatment in $Cbs^{-/-}$ mice (Figure 3G). There was no obvious change in control mice when receiving H₂S donor treatment (Figures 3A–3G). These results indicate that elevating H₂S levels are capable of restoring immune homeostasis and Treg cell numbers in $Cbs^{-/-}$ mice.

H₂S-deficiency-induced homocysteine (Hcy) accumulation might contribute to disease phenotypes in patients (Kelly et al., 2003). Because Hcy concentrations are higher in $Cbs^{-/-}$ mouse serum than in control mouse serum (Liu et al., 2014), we treated mice with Hcy and found that Hcy failed to affect Treg cell numbers (Figure S3F). These data indicate that H₂S, but not homocysteine, regulates Treg cells.
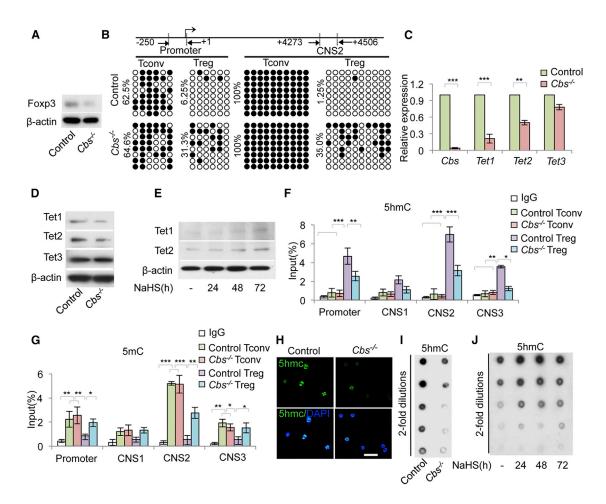
Figure 4. H₂S Targets Tet1 and Tet2 to Convert 5mC to 5hmC

(A) Foxp3 expression in control and $Cbs^{-/-}$ Treg cells are shown.

(B) The methylation status in promoter and CNS2 region of *Fopx3* in control and $Cbs^{-/-}$ CD4⁺CD25⁻ Tconv cells and Treg cells analyzed by OxBS sequencing. Each row of dots represents CpG sites in *Foxp3* promoter and CNS2 region; each dot represents a single CpG. Empty dots indicate unmethylated CpGs; black dots indicate methylated CpGs.

(C and D) The expression of Tet1, Tet2, and Tet3 in CD4⁺ T cells from control and $Cbs^{-/-}$ mice are assessed by qPCR (C) and immunoblot (D).

(E) Tet1 and Tet2 expression in CD4⁺ T cells treated with H₂S donor NaHS are shown.

(F and G) Enrichments of 5hmC (F) and 5mC (G) in *Foxp3* promoter and CNS1–3 regions are assessed by hMeDIP-qPCR and MeDIP-qPCR analysis, respectively. IgG was used as a control.

(H and I) 5hmC expression in CD4⁺ T cells are assessed by immunofluorescence staining (H) and dot blot assay analysis (I). Scale bar represents 25 μm.

(J) Global 5hmC expression in CD4⁺ T cells treated by H₂S donor NaHS are shown.

Statistical significance is determined by two-tailed Student's t tests (C) or one-way ANOVA (F and G). *$p < 0.05$, **$p < 0.01$, ***$p < 0.001$ (mean ± SD). Results are from three repeated experiments.

multiple ways, including Tet-mediated 5mC hydroxylation (Kohli and Zhang, 2013). We found that *Dnmt* expression was not altered in $Cbs^{-/-}$ CD4⁺ T cells (Figure S4E). The Tet family contributes to DNA demethylation by converting 5mC to 5hmC and has recently been implicated in epigenetic regulation of cell reprogramming and differentiation (Tahiliani et al., 2009). By immunoblot and qPCR analysis, we found that H₂S deficiency led to downregulation of Tet1 and Tet2, but not Tet3, in CD4⁺ T cells (Figures 4C, 4D, and S4F). H₂S inhibitors HA or PAG treatment resulted in downregulation of Tet1 and Tet2 in CD4⁺ T cells (Figures S4G and S4H), whereas treatment with H₂S donor NaHS rescued Tet1 and Tet2 expression in $Cbs^{-/-}$ CD4⁺ T cells (Figures 4E and S4I). These data suggest that H₂S is required for maintenance of Tet1 and Tet2 expression.

Tet-mediated active DNA demethylation within *Foxp3* might be involved in Treg cell development (Toker et al., 2013). We next investigated whether H₂S regulated 5hmC enrichment within *Foxp3* locus and found that 5hmC enrichment was decreased within *Foxp3* promoter, CNS2, and CNS3 in $Cbs^{-/-}$ Treg cells compared to the control ones, as assessed by hMeDIP-qPCR analysis (Figure 4F). In contrast, 5mC enrichment was elevated within *Foxp3* promoter, CNS2, and CNS3 in $Cbs^{-/-}$ Treg cells (Figure 4G). These data suggest that H₂S might regulate 5hmC enrichment in *Foxp3* locus. We next assessed whether H₂S modified the epigenetic landscape by affecting 5hmC levels in the genome. Dot blot assays and immunofluorescence analysis showed that global 5hmC levels were decreased in $Cbs^{-/-}$ CD4⁺ T cells (Figures 4H and 4I). More importantly,

H$_2$S donor NaHS treatment rescued global 5hmC levels in a time-dependent manner (Figure 4J). Because *Foxp3* promoter and CNS element epigenetic marks play important roles in determining Treg cell identity, we examined whether H$_2$S was required to stabilize the expression of Foxp3. We found that *Cbs*$^{-/-}$ Treg cells had reduced Foxp3 expression compared to the corresponding *Foxp3*^{GFP} Treg cells after 3 days of culture in vitro (Figure S4J). Moreover, *Cbs*$^{-/-}$ Treg cells were much easier to differentiate into Th1 and Th17 cells, but not into Th2 cells, when cultured in vitro (Figures S4K–S4M). Taken together, these data suggest that H$_2$S-mediated enrichment of 5hmC in *Foxp3* locus might contribute to Treg cell differentiation, function, and stability.

H$_2$S Regulates Tet1 and Tet2 Expression via Sulfhydration of NFYB

Tet enzyme expression is under tight transcriptional regulation. For instance, OCT4 and C/EBPα directly associate with *Tet1* and *Tet2* promoters and regulatory elements to regulate their expression in pluripotent stem cells and myeloid lineage cells (Kallin et al., 2012; Koh et al., 2011). Because analysis of *Tet1* and *Tet2* promoters (Transfec, Biobase) showed conserved CCAAT binding motif for NFY, which is a well-characterized heterotrimeric transcriptional activator (NFYA, NFYB, and NFYC), we verified that NFYB bound to the promoters of *Tet1* and *Tet2* by ChIP-qPCR analysis. This binding was decreased in *Cbs*$^{-/-}$ CD4$^+$ T cells. When treated with H$_2$S donor, but not H$_2$S substrate L-cysteine, NFYB binding to *Tet1* and *Tet2* promoters were restored in *Cbs*$^{-/-}$ T cells (Figure 5A), indicating that H$_2$S might facilitate NFYB binding to *Tet1* and *Tet2* promoters. Knockdown of *Nfyb* by siRNA led to decreased expression of Tet1 and Tet2 as well as partially suppressed H$_2$S-induced upregulation of Tet1 and Tet2 in CD4$^+$ T cells (Figures 5B, 5C, and S5A). However, we found that *Cbs*$^{-/-}$ and control cells expressed similar amounts of NFYB (Figure 5D).

Ubiquitination at Lys138 is important for NFYB transcriptional activation (Nardini et al., 2013), implying that protein modification might regulate NFYB activity. H$_2$S mediates signal response predominantly by sulfhydrating cysteines of target proteins such as GAPDH and actin, leading to augmentation of GAPDH catalytic activity and actin polymerization (Mustafa et al., 2009). Sulfhydration (SHY) is a physiological process in which H$_2$S attaches an additional sulfur to the thiol (-SH) group of a cysteine, yielding a hydropersulfide (-SSH) (Sen et al., 2012). We employed Alexa Fluor 488-conjugated C5 maleimide (green maleimide), which interacts selectively with sulfhydryl groups of cysteines, to label both sulfhydrated and unsulfhydrated cysteines. Dithiothreitol (DTT) treatment was used to selectively cleave disulfide bonds and detach the green signal from sulfhydrated protein only, resulting in decreased fluorescence (Figure 5E). We used the green maleimide to detect overall protein sulfhydration in T cell lysates. In control T cells, we detected green bands representing proteins with SH and SSH in the presence of L-cysteine and observed a 50% reduction of the green signal after DTT treatment. Green signals were also detected in *Cbs*$^{-/-}$ T cells; however, DTT treatment failed to reduce the green signals (Figure S5B). DTT treatment abolished the green NFYB signal in the presence of L-cysteine in control T cells, indicating sulfhydration of NFYB. In contrast, in *Cbs*$^{-/-}$ T cells, DTT did not affect the green NFYB signal, indicating absence of NFYB sulfhydration in *Cbs*$^{-/-}$ T cells (Figure 5F). Treatment with H$_2$S donor NaHS improved sulfhydration of NFYB in control T cells and also restored sulfhydration of NFYB in *Cbs*$^{-/-}$ T cells (Figure 5G). We next employed liquid chromatography-mass spectrometric analysis (LC-MS) to identify the cysteine residue responsible for sulfhydration of NFYB under H$_2$S donor treatment (Liu et al., 2014). The mass shift suggested that the cysteine residues (C) were sulfhydrated at the C105 site of NFYB after H$_2$S donor treatment (Figures 5H and S5C). To verify the effect of sulfhydration on NFYB binding to *Tet1* and *Tet2* activity, we used diamide (DM), which is capable of reducing the number of sulfhydryls and thereby reducing protein sulfhydration (Kosower et al., 1969), to pretreat *Cbs*$^{-/-}$ T cells. ChIP-qPCR results showed that DM treatment blocked H$_2$S donor-induced rescue of NFYB binding to *Tet1* and *Tet2* promoters (Figure 5I). To further confirm that sulfyhydration of NFYB cysteine residues played a critical role in H$_2$S-mediated Tet1 and Tet2 expression, we generated *Nfyb* C105 mutation constructs (*Nfyb* C105A) and overexpressed *Nfyb* and *Nfyb* C105A in CD4$^+$ T cells (Figures 5J and S5D). Overexpression of *Nfyb* elevated Tet1 and Tet2 expression, especially under H$_2$S donor treatment (Figures 5K and 5L). However, overexpression of *Nfyb* C105A failed to upregulate expression of Tet1 and Tet2 either with or without H$_2$S donor treatment (Figures 5K and 5L), indicating that H$_2$S-regulated Tet1 and Tet2 expression in CD4$^+$ T cells depends at least partially on the sulfhydration of NFYB C105. These results suggest that H$_2$S-mediated sulfhydration of NFYB is important for NFY complex binding to *Tet1* and *Tet2* promoters to regulate their expression.

Loss of Tet1 and Tet2 Impair Treg Cell Differentiation and Function

In order to verify the role of Tet1 and Tet2 in immune homeostasis and Treg cell differentiation and function, we generated *Tet1*$^{-/-}$*Cd4*^{Cre}*Tet2*$^{fl/fl}$ double knockout (*Tet* DKO) mice (Figure S6A) and found that they developed inflammation in multiple organs, including the colon, lung, and liver (Figure 6A), along with infiltration of abundant CD3-positive cells (Figure S6B), decreased body weight (Figure S6C), and several elevated autoreactive antibodies, including anti-dsDNA IgG (Figure 6B) and IgM (Figure 6C) antibodies, and ANA (Figure 6D) in the peripheral blood. Treg cell frequencies in *Tet* DKO mice were significantly decreased in spleen and lymph nodes compared to the control group (Figure 6E). In addition, total numbers of Treg cells were decreased in *Tet* DKO mice (Figure 6F). *Tet* DKO Treg cells also showed reduced Foxp3 expression (Figures 6G–6I). These results indicate that *Tet1* and *Tet2* depletion led to reduction of Treg cell frequency and Foxp3 expression. The proportion of Treg cells was also consistently decreased in the lung and liver in *Tet* DKO mice (Figure S6D). Moreover, Treg cells from *Tet* DKO mice showed reduced capacity to suppress CD4$^+$CD25$^-$ cells, as assessed by in vitro coculture assay (Figure 6J). The experimental data imply that Tet1 and Tet2 are required for maintenance of immune homeostasis and Treg cell differentiation and function.

Next, we generated mixed bone marrow chimeras to confirm the intrinsic role of Tet1 and Tet2 in CD4$^+$Foxp3$^+$ Treg cell generation. We injected C57BL/6 (CD45.1$^+$) bone marrow with *Tet* DKO (CD45.2$^+$) bone marrow into sublethally irradiated WT
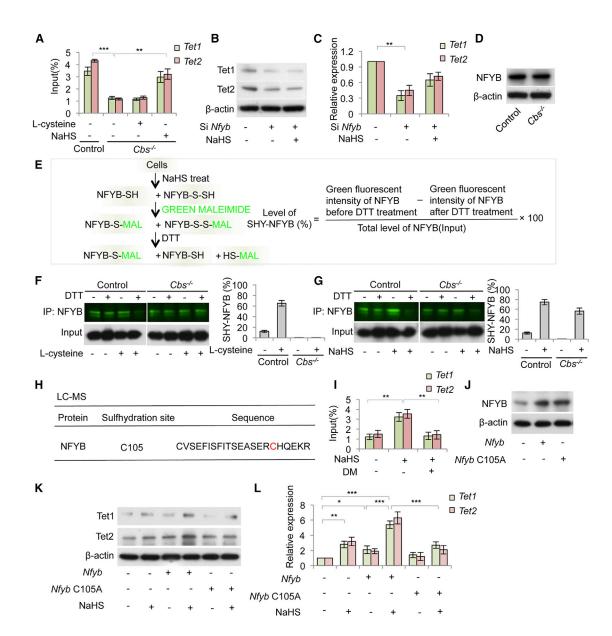
Figure 5. H$_2$S Regulates Tet1 and Tet2 Expression via Sulfhydration of NFYB

(A) NFYB enrichments in the promoters of *Tet1* and *Tet2* are analyzed by ChIP-qPCR.

(B and C) The expression of Tet1 and Tet2 in CD4$^+$ T cells after indicated treatment are assessed by immunoblot (B) and qPCR (C).

(D) Immunoblot demonstrating NFYB expression in control and *Cbs$^{-/-}$* T cells.

(E) Schematic diagram for detection of NFYB sulfhydration with green maleimide.

(F and G) The green signal of NFYB protein after indicated treatment (L-cysteine in F and NaHS in G) in control and *Cbs$^{-/-}$* T cells.

(H) LC-MS analysis of sulfhydration in NFYB protein Cys105 after NaHS (1 mM) treatment.

(I) ChIP-qPCR analyzes NFYB enrichment in the promoters of *Tet1* and *Tet2* in *Cbs$^{-/-}$* T cells in indicated treatments.

(J) NFYB expression in CD4$^+$ T cells without or with *Nfyb* or *Nfyb* C105A plasmids transfection are analyzed by immunoblot.

(K and L) The expression of Tet1 and Tet2 in CD4$^+$ T cells after indicated treatments are assessed by immunoblot (K) and qPCR (L).

Statistical significance is by one-way ANOVA (A, C, I, L). **$p < 0.05$, **$p < 0.01$, ***$p < 0.001$ (mean ± SD). Results are from three repeated experiments.

recipient mice. We revealed that the recipient mice had a reduced proportion and number of CD4$^+$Foxp3$^+$ Treg cells originating from *Tet* DKO mouse bone marrow compared to those originating from the control ones (Figures 6K and 6L), indicating that Tet1 and Tet2 intrinsically regulate Treg cell differentiation. T cells from *Tet* DKO mice displayed slightly decreased Treg cell differentiation in the presence of TGF-β and IL-2 (Figure S6E).

Furthermore, *Tet1* and *Tet2* depletion resulted in reduced global 5hmC levels in CD4$^+$ T cells (Figure S6F) and 5hmC enrichment within *Foxp3* promoter, as well as CNS2 and CNS3 in Treg cells, as assessed by hMeDIP-qPCR (Figure 6M). The enrichment of 5mC within *Foxp3* promoter and CNS2 were elevated in *Tet* DKO Treg cells, as assessed by MeDIP-qPCR (Figure 6N). We found that Tconv cells from both *Tet* DKO and control mice
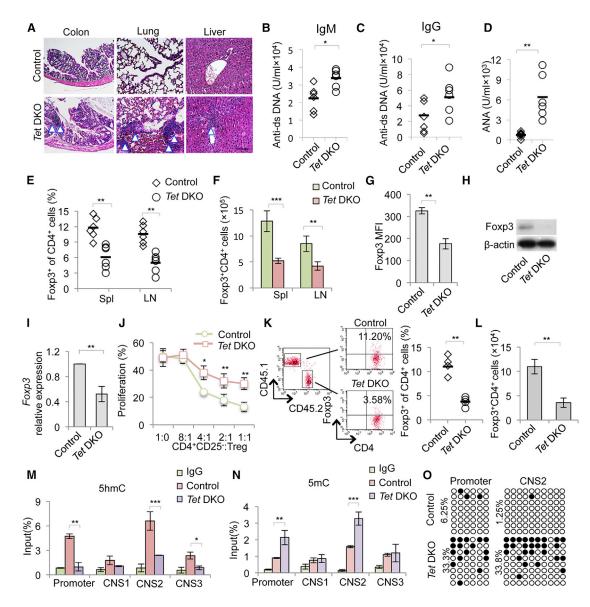
Figure 6. Tet1 and Tet2 Are Required for Treg Cell Differentiation and Function

(A) HE staining show inflammatory cell infiltration (blue triangle) in the colon, lung, and liver of $Tet1^{-/-}Cd4^{Cre}Tet2^{fl/fl}$ (Tet DKO) mice; $Tet2^{fl/fl}$ mice are used as control. Scale bar represents 100 μm.

(B–D) The anti-dsDNA antibodies IgM (B) and IgG (C) and anti-ANA (D) are measured by ELISA in control and Tet DKO mouse serum.

(E) Treg cell frequencies in the spleen (Spl) and lymph nodes (LN) from control and Tet DKO mice are shown.

(F) The total numbers of Foxp3$^+$ Treg cells are shown.

(G–I) Foxp3 expression in control and Tet DKO Treg cells are assessed by flow cytometry (G), immunoblot (H), and qPCR (I).

(J) Suppressive capacities of Tet DKO Treg cells and control ones are shown.

(K and L) WT control (CD45.1) and Tet DKO (CD45.2) bone marrow cells co-transferred into sublethally irradiated WT recipient mice (n = 4) for 6 weeks to generate mixed bone marrow chimeric mice. Representative flow cytometry plots of splenic CD45.1 and CD45.2 cells are shown. Percentages (K) and numbers (L) of CD4$^+$Foxp3$^+$ Treg cells are shown.

(M and N) Enrichments of 5hmC (M) and 5mC (N) within Foxp3 promoter and CNS1–3 regions in control and Tet DKO Treg cells are assessed by hMeDIP-qPCR and MeDIP-qPCR analysis, respectively. IgG is used as a control.

(O) OxBS-sequencing analysis shows the promoter and CNS2 region methylation status of Foxp3 in Treg cells.

Statistical significance is determined by two-tailed Student's t tests (B–G, I–L) and one-way ANOVA (M and N). *p < 0.05, **p < 0.01, ***p < 0.001 (mean ± SD). Results are from three repeated experiments.

were high methylated in the Foxp3 promoter and CNS2 region, and Tet1 and Tet2 depletion resulted in reduced DNA demethylation in T cells compared to controls (Figures 6O and S6G). Similar to $Cbs^{-/-}$ Treg cells, Tet1- and Tet2-depleted Treg cells

expressed reduced amounts of Foxp3 after 3 days in vitro culture. Tet DKO Treg cells were much easier to differentiate into Th1 and Th17 cells, but not into Th2 cells, when cultured in vitro (Figures S6H–S6K).

To verify the role of Tet1 and Tet2 in Treg cell differentiation and function, we showed that WT control Treg cells adaptively transferred into *Tet* DKO mice were capable of ameliorating systemic inflammatory phenotypes, as shown by reduction of the elevated levels of autoreactive antibodies, improvement of histopathological alteration in the colon, liver, and lung, elevation of the body weight, and extension of mouse lifespan (Figures S6L–S6Q). We next generated $Tet1^{-/-}Foxp3^{Cre}Tet2^{fl/fl}$ double knockout (*Tet* KO) mice and found that these mice developed similar inflammation phenotypes to those observed in *Tet* DKO mice, such as multiple organ inflammation, elevated autoreactive antibodies, decreased body weight, and higher incidence of death (Figures S6L–S6Q). In addition, *Tet* KO mice showed decreased Treg cell frequency and Foxp3 expression in Treg cells (Figures S6R and S6S). Taken together, these results indicate that Tet1 and Tet2 are required for *Foxp3* demethylation and Treg cell differentiation and function.

Smad3 and Stat5 Recruit Tet Proteins to *Foxp3* Locus

Previous studies showed that 5hmC colocalized with Tet1 at high and intermediate GpG-content sequences (Xu et al., 2011). To investigate whether *Foxp3* is a direct target of Tet1 and Tet2, we showed that Tet1 and Tet2 bound to *Foxp3* promoter and CNS1–3 regions with different enrichment levels, which were decreased in $Cbs^{-/-}$ Treg cells compared to the control group (Figure 7A). Because TGF-β and IL-2 play indispensable roles in Treg cell development, differentiation, and cell identity (Chen et al., 2003; Feng et al., 2014; Konkel et al., 2014; Li et al., 2014), we examined whether TGF-β and IL-2 signaling regulate Tet1 and Tet2 expression and found that TGF-β and IL-2 treatment failed to affect expression of Tet1 and Tet2 or global 5hmC levels in T cells (Figures 7B and 7C). Because Tet1 and Tet2 can interact with other molecules, such as NANOG, to synergistically regulate cell signaling for reprogramming (Costa et al., 2013), we assessed whether TGF-β and IL-2 treatment regulated Tet1 and Tet2 interaction with protein complexes in T cells. We used LC-MS analysis to show that Smad3 and Stat5a interacted with both Tet1 and Tet2 in CD4$^+$ T cells and Treg cells (Figures S7A–S7C, Table S1). Next, we performed immunoprecipitation to show that Tet1 and Tet2 co-immunoprecipitated with Smad3 and Stat5 to a higher degree in Treg cells compared to CD4$^+$ T cells. TGF-β and IL-2 treatment enhanced co-immunoprecipitation of Smad3 and Stat5 with Tet1 and Tet2 in T cells whereas TGF-β- and IL-2-neutralizing antibody attenuated the co-immunoprecipitation of Smad3 and Stat5 with Tet1 and Tet2 in Treg cells (Figure 7D). Stat5 binds to *Foxp3* promoter and CNS2 region, serving as a key regulator to open CNS2 region to maintain Treg cell identity, and CNS1 is a TGF-β-sensitive element that contains binding sites for NFAT and SMADs (Feng et al., 2014; Ogawa et al., 2014). Treg cells showed higher enrichment of Tet1 and Tet2 on *Foxp3* promoter and CNS2 compared to CD4$^+$ T cells (Figures 7E and 7F). To determine the role of TGF-β and IL-2 in regulating Tet1 and Tet2 binding to *Foxp3* locus, we showed that TGF-β and IL-2 treatment elevated Tet1 and Tet2 binding to *Foxp3* promoter, CNS1 and CNS2, but not CNS3 in CD4$^+$ T cells, whereas TGF-β- and IL-2-neutralizing antibody treatment abolished Tet1 and Tet2 binding to *Foxp3* locus in Treg cells (Figures 7E and 7F). To

verify the roles of protein interaction and recruitment in *Foxp3* demethylation, CD4$^+$CD25$^-$Foxp3^{GFP-} T cells from control or *Tet* DKO mice were transferred to $Rag1^{-/-}$ mice and a fraction of CD4$^+$Foxp3^{GFP+} cells were generated. These cells showed progressive demethylation of *Foxp3* promoter and CNS2 regions (Figure 7G). Moreover, CD4$^+$Foxp3^{GFP+} from the *Tet* DKO T cell transfer group showed reduced demethylation compared to the control group at *Foxp3* promoter and CNS2 region. Smad3 and Stat5 knockdown decreased demethylation of *Foxp3* promoter and CNS2 compared to the scramble control group (Figures 7G and S7D). Taken together, these findings indicate that TGF-β and IL-2 activated Smad3 and Stat5, recruiting Tet1 and Tet2 binding to *Foxp3* locus to regulate *Foxp3* demethylation and Treg cell differentiation and function.

H₂S Donor Treatment Rescues Treg Cell Deficiency in $Cbs^{-/-}$ Mice in a Tet-Dependent Manner

We next examined whether rescue of Treg cell deficiency by H₂S donor depended on Tet1 and Tet2 and found that H₂S donor NaHS treatment failed to rescue Treg cell number decrease in *Tet* DKO mice (Figure 7H). When we infused *Tet1*- and *Tet2*-overexpressed CD4$^+$CD25$^-$Foxp3^{GFP-} T cells to $Rag1^{-/-}$ mice, the *Tet1* and *Tet2* overexpression group had an increased numbers of CD4$^+$Foxp3$^+$ Treg cells relative to the control group (Figures 7I and S7E). We further analyzed Tet1 and Tet2 expression in CD4$^+$ T cells from H₂S donor GYY4137 injection mice and found that Tet1 and Tet2 was elevated after GYY4137 treatment in $Cbs^{-/-}$ mice (Figures 7J and S7F). HMeDIP-qPCR analysis showed that GYY4137 injection elevated 5hmC enrichment within the *Foxp3* locus in Treg cells from $Cbs^{-/-}$ mice (Figure 7K). These data indicate that the role of H₂S in regulating Treg cell differentiation and function depends on Tet-mediated demethylation.

DISCUSSION

We showed that reduced levels of H₂S were responsible for the impairment of CD4$^+$Foxp3$^+$ Treg cell differentiation and function and systemic autoimmune disease observed in mice. Administration of H₂S donor could rescue Treg-cell-deficient and systemic autoimmune phenotypes in $Cbs^{-/-}$ mice and WT Treg cell infusion could also partially rescue autoimmunity in $Cbs^{-/-}$ mice, suggesting that H₂S is indispensable for Treg-cell-associated immune homeostasis.

Epigenetic modifications, especially DNA methylation, play an important role in immune system and Foxp3$^+$ Treg cell differentiation and lineage stabilization (Ichiyama et al., 2015; Kim and Leonard, 2007; Tsagaratou et al., 2014). Tet expression is important for *Foxp3* demethylation in the thymus and peripheral Treg cells and might play an essential role in Treg cell development, differentiation, and function as well as the maintenance of immune homeostasis (Nair and Oh, 2014; Toker et al., 2013; Wang et al., 2013). Our results showed that deletion of *Tet1* and *Tet2* resulted in systemic autoimmune disease due to a substantial reduction and impairment of Treg cell differentiation and function. *Tet*-deleted Treg cells showed substantially reduced enrichment of 5hmC within *Foxp3* promoter and CNS elements, which might be responsible for
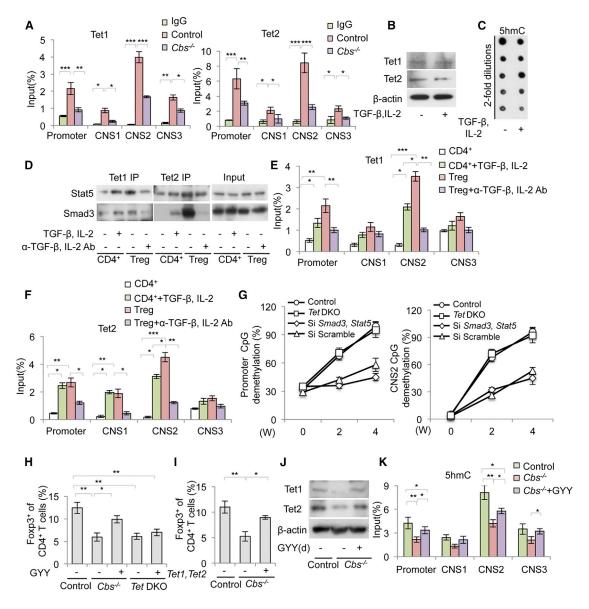
Figure 7. Activated Smad3 and Stat5 Recruit Tet1 and Tet2 Binding to *Foxp3* Locus

(A) ChIP-qPCR analyzes Tet1 and Tet2 binding in the promoter and CNS regions of *Foxp3* in Treg cells. IgG is used as control.

(B and C) Tet1 and Tet2 expression (B) and global 5hmC levels (C) in CD4^{+} T cells treated with TGF-β and IL-2 are assessed by immunoblot and dot blot assay, respectively.

(D) Tet1 and Tet2 interaction with Smad3 and Stat5 in CD4^{+} T cells and Treg cells by indicated treatments are assessed by protein complex immunoprecipitation (Co-IP) assay.

(E and F) Tet1 (E) and Tet2 (F) binding activity to the promoter and CNS1-3 regions of *Foxp3* in CD4^{+} T cells and Treg cells are analyzed by ChIP-qPCR.

(G) CD4^{+}CD25^{−}Foxp3[GFP−] T cells from control and *Tet* DKO mice are transferred into *Rag1*^{−/−} mice (n = 4). The generated CD4^{+}Foxp3[GFP+] cells are isolated for methylation analysis and show the demethylation ratios of *Foxp3* promoter and CNS2 in indicated groups.

(H) Treg cell frequencies in *Cbs*^{−/−} mice (n = 4) and *Tet* DKO mice (n = 4) with or without GYY4137 (GYY) injection (n = 4) are shown, as assessed by flow cytometry.

(I) Treg cell frequency in *Rag1*^{−/−} mice (n = 4) after transferring control, *CBS*^{−/−}, or *Tet1*- and *Tet2*-overexpressed *Cbs*^{−/−} CD4^{+} naive T cells, as assessed by flow cytometry.

(J) Tet1 and Tet2 expression in CD4^{+} T cells after GYY4137 injection in *Cbs*^{−/−} mice are shown.

(K) 5hmC enrichment within the promoter and CNS1–3 regions of *Foxp3* in Treg cells with or without GYY4137 injection in *Cbs*^{−/−} mice are analyzed by hMeDIP-qPCR.

Statistical significance is determined by one-way ANOVA (A, E, F, H, I, K). *$p < 0.05$, **$p < 0.01$, ***$p < 0.001$ (mean ± SD). Results are from three repeated experiments.

Treg cell deficiency. However, whether Tet family members regulate other types of cells in the immune system still needs further investigation. DNA methylation and demethylation are regulated by multiple factors (Wu and Zhang, 2014). $Cbs^{-/-}$ and Tet DKO Treg cells showed hypermethylation at $Foxp3$ promoter and CNS2, with variable methylation ratio per cell. Based on Foxp3 expression, Treg cells can be classified into Foxp3^{lo}, Fopx3^{med}, and Foxp3^{hi} subsets. Among these, the Foxp3^{lo} subset was substantially reduced in $Foxp3$ CNS2 knockout mice (Li et al., 2014), implying that different Treg cell subsets might be regulated differently based on $Foxp3$ expression or methylation.

The H$_2$S-medidated protein sulfhydration might affect its regulatory effects on inflammatory processes and vasorelaxation (Paul and Snyder, 2012). H$_2$S could sulfhydrate NFYB to control its binding activity to $Tet1$ and $Tet2$ promoters, and thus regulate Tet1 and Tet2 expression in Treg cells. This might illustrate the underlying mechanism of how sulfhydration was involved in inflammatory processes. Strikingly, H$_2$S-mediated sulfhydration might represent a new protein modification approach to regulate NFYB function, similar to the ubiquitination of NFYB at Lys138 to regulate transcriptional activation (Nardini et al., 2013). H$_2$S affected sulfhydration of NFYB to control NFYB complex binding to the promoters of $Tet1$ and $Tet2$, forming a H$_2$S-NFYB-Tet axis, thus regulating Treg cell differentiation and function. Tet-mediated 5mC hydroxylation has been detected in a broad range of cell types and extensively studied in embryonic stem cells (ESCs), brain cells, and neurons (Kriaucionis and Heintz, 2009; Tahiliani et al., 2009). H$_2$S exerts multifaceted and important effects on the central nervous system and NFY is required for maintenance of ESC properties and neuronal cell functions (Grskovic et al., 2007; Yamanaka et al., 2014). These pieces of evidence suggest that the H$_2$S-NFYB-Tet regulation cascade might be applicable to other cell types.

Tet1 binds to target genes either to regulate the metabolism of 5mC at CpG-rich sequences by converting it to 5hmC or to regulate transcription. For example, Tet1 is involved in transcriptional repression through its interaction with the SIN3A complex (Williams et al., 2011) and establishes cell pluripotency through its interaction with NANOG (Costa et al., 2013). We showed that phosphorylated Smad3 and Stat5, upon stimulation by TGF-β and IL-2, facilitated Tet1 and Tet2 binding to $Foxp3$ locus. This was achieved via the formation of a protein complex, leading to the enrichment of 5hmC to promote Foxp3 expression and Treg cell differentiation and function. Stable Treg cell lineage establishment requires concurrent expression of the transcription factor Foxp3 and establishment of Treg-cell-specific hypomethylation pattern (Ohkura et al., 2012). Our study indicates that Treg cell lineage determination and maintenance require synergistic regulation by signaling pathway and epigenetic modification, in which Tet1 and Tet2 are required for the dynamic process that establishes and maintains hypomethylation of $Foxp3$.

In conclusion, physiological levels of H$_2$S are required to maintain immune homeostasis by regulating Tet expression in T cells. Treg cell lineage determination and maintenance require synergistic regulation by signaling pathway and epigenetic modification.

EXPERIMENTAL PROCEDURES

Mice

C57BL/6 (JAX #000664), B6.SJL-Ptprc^a (JAX #002014, CD45.1$^+$), B6.129S7-$Rag1^{tm1Mom}$/J (JAX #002216, $Rag1^{-/-}$), B6.129P2-Cbs^{tm1Unc}/J (JAX #002461, $Cbs^{+/-}$), B6.Cg-Foxp3^{tm2Tch}/J (JAX #006772, $Foxp3^{GFP}$), B6.129S4-$Tet1^{tm1.1Jae}$/J (JAX #017358, $Tet1^{+/-}$), B6.129S-$Tet2^{tm1.1Iaai}$/J (JAX #017573, $Tet2^{fl/fl}$), and Tg (Cd4-cre)1Cwi/BfluJ (JAX #017336, $Cd4^{Cre}$) mice were purchased from Jackson Lab. To generate $Cbs^{-/-}Foxp3^{GFP}$ mice, we mated $Cbs^{+/-}$ mice with $Cbs^{+/-}Foxp3^{GFP}$ mice. To generate $Tet1^{-/-}Cd4^{Cre}Tet2^{fl/fl}$ mice, we mated $Tet1^{+/-}Cd4^{Cre}Tet2^{fl/+}$ mice with $Tet1^{+/-}Tet2^{fl/fl}$ mice. To generate $Tet1^{-/-}Cd4^{Cre}Tet2^{fl/fl}Foxp3^{GFP}$ mice, we mated $Tet1^{+/-}Cd4^{Cre}Tet2^{fl/+}Foxp3^{GFP}$ mice with $Tet1^{+/-}Tet2^{fl/fl}$ mice. All animal experiments were performed under institutionally approved protocols for the use of animal research at the University of Southern California (USC#11141, 11953, and 11327) and University of Pennsylvania (IACUC# 805478).

Adoptive Transfer Colitis

$Rag1^{-/-}$ mice were injected intravenously with 4×10^5 FACS-sorted naive CD4$^+$CD25$^-$CD45RB^{hi} cells from control or $Cbs^{-/-}$ mice, without or with control or $Cbs^{-/-}$ 2×10^5 Treg cells. After T cell reconstitution, mice were monitored weekly and samples were harvested 6 weeks later for further investigation.

Generation of Mixed Bone Marrow Chimeric Mice

Bone marrow cells were isolated from femurs and tibias of donor animals ($Tet1^{-/-}Cd4^{Cre}Tet2^{fl/fl}$ CD45.2 or $Cbs^{-/-}$ CD45.2 and WT CD45.1). C57BL/6 WT mice received sublethal irradiation (10 Gy). At 6 hr after irradiation, $Tet1^{-/-}Cd4^{Cre}Tet2^{fl/fl}$ CD45.2 cells (1×10^6) or $Cbs^{-/-}$ CD45.2 cells (1×10^6) and WT CD45.1 cells (1×10^6) were infused into irradiated C57BL/6 WT mice. Eight weeks later, mice were sacrificed and analyzed via flow cytometry.

Dot Blot Assay

DNA was diluted to 100 ng/μl and a dilution series was performed; then, 1 μl was spotted on a 0.45 μm pore size positively charged nylon membrane. The membrane was air-dried completely on a paper towel for 10 min at room temperature, followed by baking in a vacuum oven (80°C) for 2 hr. The membrane was blocked in 5% milk/TBS/0.1%Tween-20 for 1 hr, followed by incubation with 5hmC or 5mC antibodies in TBST/0.1% BSA overnight at 4°C overnight. Then they were treated with horseradish peroxidase-conjugated rabbit or mouse IgG (Santa Cruz) (1:10,000) for 1 hr, enhanced with a SuperSignal West Pico Chemiluminescent Substrate (Pierce), and exposed on BIOMAX MR films (Kodak).

Microarray

Total RNAs were extracted from control and $Cbs^{-/-}$ CD4$^+$ T cells with an RNeasy kit (QIAGEN). Microarray assays were performed at the Genome Center of Children's Hospital, Los Angeles, using Mouse Gene 1.0 ST arrays (Affymetrix). The global gene expression difference was analyzed by Partek Genomics Suite and Ingenuity Pathway Analysis (IPA) software. Global gene expression profiles rank ordered by relative fold-change values were analyzed using Gene Set Enrichment Analysis software (Broad Institute, MIT).

Statistical Analysis

Significance was determined by independent two-tailed Student's t tests or one-way analysis of variance (ANOVA) using SPSS 18.0 software. Kaplan-Meier survival curves were constructed and analyzed by a log-rank test. At least four mice were randomly assigned to each group. Exact number of mice used in each group was indicated in the figure legends. Data were assessed for normal distribution and similar variance between groups prior to further statistical analysis. p values less than 0.05 were considered significant.

ACCESSION NUMBERS

The Gene Expression Omnibus accession number for control and $Cbs^{-/-}$ CD4$^+$ T cell microarray data is GEO: GSE59241.

REFERENCES

Chen, W., Jin, W., Hardegen, N., Lei, K.J., Li, L., Marinos, N., McGrady, G., and Wahl, S.M. (2003). Conversion of peripheral CD4+CD25− naive T cells to CD4+CD25+ regulatory T cells by TGF-beta induction of transcription factor Foxp3. J. Exp. Med. 198, 1875–1886.

Costa, Y., Ding, J., Theunissen, T.W., Faiola, F., Hore, T.A., Shliaha, P.V., Fidalgo, M., Saunders, A., Lawrence, M., Dietmann, S., et al. (2013). NANOG-dependent function of TET1 and TET2 in establishment of pluripotency. Nature 495, 370–374.

Feng, Y., Arvey, A., Chinen, T., van der Veeken, J., Gasteiger, G., and Rudensky, A.Y. (2014). Control of the inheritance of regulatory T cell identity by a cis element in the Foxp3 locus. Cell 158, 749–763.

Fiorucci, S., Orlandi, S., Mencarelli, A., Caliendo, G., Santagada, V., Distrutti, E., Santucci, L., Cirino, G., and Wallace, J.L. (2007). Enhanced activity of a hydrogen sulphide-releasing derivative of mesalamine (ATB-429) in a mouse model of colitis. Br. J. Pharmacol. 150, 996–1002.

Floess, S., Freyer, J., Siewert, C., Baron, U., Olek, S., Polansky, J., Schlawe, K., Chang, H.D., Bopp, T., Schmitt, E., et al. (2007). Epigenetic control of the foxp3 locus in regulatory T cells. PLoS Biol. 5, e38.

Grskovic, M., Chaivorapol, C., Gaspar-Maia, A., Li, H., and Ramalho-Santos, M. (2007). Systematic identification of cis-regulatory sequences active in mouse and human embryonic stem cells. PLoS Genet. 3, e145.

Han, Y., Zeng, F., Tan, G., Yang, C., Tang, H., Luo, Y., Feng, J., Xiong, H., and Guo, Q. (2013). Hydrogen sulfide inhibits abnormal proliferation of lymphocytes via AKT/GSK3β signal pathway in systemic lupus erythematosus patients. Cell. Physiol. Biochem. 31, 795–804.

Hori, S., Nomura, T., and Sakaguchi, S. (2003). Control of regulatory T cell development by the transcription factor Foxp3. Science 299, 1057–1061.

Ichiyama, K., Chen, T., Wang, X., Yan, X., Kim, B.S., Tanaka, S., Ndiaye-Lobry, D., Deng, Y., Zou, Y., Zheng, P., et al. (2015). The methylcytosine dioxygenase Tet2 promotes DNA demethylation and activation of cytokine gene expression in T cells. Immunity 42, 613–626.

Kallin, E.M., Rodríguez-Ubreva, J., Christensen, J., Cimmino, L., Aifantis, I., Helin, K., Ballestar, E., and Graf, T. (2012). Tet2 facilitates the derepression of myeloid target genes during CEBPα-induced transdifferentiation of pre-B cells. Mol. Cell 48, 266–276.

Kelly, P.J., Furie, K.L., Kistler, J.P., Barron, M., Picard, E.H., Mandell, R., and Shih, V.E. (2003). Stroke in young patients with hyperhomocysteinemia due to cystathionine beta-synthase deficiency. Neurology 60, 275–279.

Kim, H.P., and Leonard, W.J. (2007). CREB/ATF-dependent T cell receptor-induced FoxP3 gene expression: a role for DNA methylation. J. Exp. Med. 204, 1543–1551.

Koh, K.P., Yabuuchi, A., Rao, S., Huang, Y., Cunniff, K., Nardone, J., Laiho, A., Tahiliani, M., Sommer, C.A., Mostoslavsky, G., et al. (2011). Tet1 and Tet2 regulate 5-hydroxymethylcytosine production and cell lineage specification in mouse embryonic stem cells. Cell Stem Cell 8, 200–213.

Kohli, R.M., and Zhang, Y. (2013). TET enzymes, TDG and the dynamics of DNA demethylation. Nature 502, 472–479.

Konkel, J.E., Jin, W., Abbatiello, B., Grainger, J.R., and Chen, W. (2014). Thymocyte apoptosis drives the intrathymic generation of regulatory T cells. Proc. Natl. Acad. Sci. USA 111, E465–E473.

Kosower, N.S., Kosower, E.M., Wertheim, B., and Correa, W.S. (1969). Diamide, a new reagent for the intracellular oxidation of glutathione to the disulfide. Biochem. Biophys. Res. Commun. 37, 593–596.

Kriaucionis, S., and Heintz, N. (2009). The nuclear DNA base 5-hydroxymethyl-cytosine is present in Purkinje neurons and the brain. Science 324, 929–930.

Li, L., Bhatia, M., Zhu, Y.Z., Zhu, Y.C., Ramnath, R.D., Wang, Z.J., Anuar, F.B., Whiteman, M., Salto-Tellez, M., and Moore, P.K. (2005). Hydrogen sulfide is a novel mediator of lipopolysaccharide-induced inflammation in the mouse. FASEB J. 19, 1196–1198.

Li, X., Liang, Y., LeBlanc, M., Benner, C., and Zheng, Y. (2014). Function of a Foxp3 cis-element in protecting regulatory T cell identity. Cell 158, 734–748.

Liu, Y., Yang, R., Liu, X., Zhou, Y., Qu, C., Kikuiri, T., Wang, S., Zandi, E., Du, J., Ambudkar, I.S., and Shi, S. (2014). Hydrogen sulfide maintains mesenchymal stem cell function and bone homeostasis via regulation of Ca(2+) channel sulfhydration. Cell Stem Cell 15, 66–78.

Mustafa, A.K., Gadalla, M.M., Sen, N., Kim, S., Mu, W., Gazi, S.K., Barrow, R.K., Yang, G., Wang, R., and Snyder, S.H. (2009). H2S signals through protein S-sulfhydration. Sci. Signal. 2, ra72.

Nair, V.S., and Oh, K.I. (2014). Down-regulation of Tet2 prevents TSDR demethylation in IL2 deficient regulatory T cells. Biochem. Biophys. Res. Commun. 450, 918–924.

Nardini, M., Gnesutta, N., Donati, G., Gatta, R., Forni, C., Fossati, A., Vonrhein, C., Moras, D., Romier, C., Bolognesi, M., and Mantovani, R. (2013). Sequence-specific transcription factor NF-Y displays histone-like DNA binding and H2B-like ubiquitination. Cell 152, 132–143.

Ogawa, C., Tone, Y., Tsuda, M., Peter, C., Waldmann, H., and Tone, M. (2014). TGF-β-mediated Foxp3 gene expression is cooperatively regulated by Stat5, Creb, and AP-1 through CNS2. J. Immunol. 192, 475–483.

Ohkura, N., Hamaguchi, M., Morikawa, H., Sugimura, K., Tanaka, A., Ito, Y., Osaki, M., Tanaka, Y., Yamashita, R., Nakano, N., et al. (2012). T cell receptor stimulation-induced epigenetic changes and Foxp3 expression are independent and complementary events required for Treg cell development. Immunity 37, 785–799.

Paul, B.D., and Snyder, S.H. (2012). H2S signalling through protein sulfhydration and beyond. Nat. Rev. Mol. Cell Biol. 13, 499–507.

Peng, Y.J., Makarenko, V.V., Nanduri, J., Vasavda, C., Raghuraman, G., Yuan, G., Gadalla, M.M., Kumar, G.K., Snyder, S.H., and Prabhakar, N.R. (2014). Inherent variations in CO-H2S-mediated carotid body O2 sensing mediate hypertension and pulmonary edema. Proc. Natl. Acad. Sci. USA 111, 1174–1179.

Sen, N., Paul, B.D., Gadalla, M.M., Mustafa, A.K., Sen, T., Xu, R., Kim, S., and Snyder, S.H. (2012). Hydrogen sulfide-linked sulfhydration of NF-κB mediates its antiapoptotic actions. Mol. Cell 45, 13–24.

Shevach, E.M. (2000). Regulatory T cells in autoimmmunity. Annu. Rev. Immunol. 18, 423–449.

Song, S.J., Poliseno, L., Song, M.S., Ala, U., Webster, K., Ng, C., Beringer, G., Brikbak, N.J., Yuan, X., Cantley, L.C., et al. (2013). MicroRNA-antagonism regulates breast cancer stemness and metastasis via TET-family-dependent chromatin remodeling. Cell 154, 311–324.

Szabo, C., Coletta, C., Chao, C., Módis, K., Szczesny, B., Papapetropoulos, A., and Hellmich, M.R. (2013). Tumor-derived hydrogen sulfide, produced by cystathionine-β-synthase, stimulates bioenergetics, cell proliferation, and angiogenesis in colon cancer. Proc. Natl. Acad. Sci. USA *110*, 12474–12479.

Tahiliani, M., Koh, K.P., Shen, Y., Pastor, W.A., Bandukwala, H., Brudno, Y., Agarwal, S., Iyer, L.M., Liu, D.R., Aravind, L., and Rao, A. (2009). Conversion of 5-methylcytosine to 5-hydroxymethylcytosine in mammalian DNA by MLL partner TET1. Science *324*, 930–935.

Toker, A., Engelbert, D., Garg, G., Polansky, J.K., Floess, S., Miyao, T., Baron, U., Düber, S., Geffers, R., Giehr, P., et al. (2013). Active demethylation of the Foxp3 locus leads to the generation of stable regulatory T cells within the thymus. J. Immunol. *190*, 3180–3188.

Tsagaratou, A., Äijö, T., Lio, C.W., Yue, X., Huang, Y., Jacobsen, S.E., Lähdesmäki, H., and Rao, A. (2014). Dissecting the dynamic changes of 5-hydroxymethylcytosine in T-cell development and differentiation. Proc. Natl. Acad. Sci. USA *111*, E3306–E3315.

Vignali, D.A., Collison, L.W., and Workman, C.J. (2008). How regulatory T cells work. Nat. Rev. Immunol. *8*, 523–532.

Wang, R. (2002). Two's company, three's a crowd: can H_2S be the third endogenous gaseous transmitter? FASEB J. *16*, 1792–1798.

Wang, L., Liu, Y., Han, R., Beier, U.H., Thomas, R.M., Wells, A.D., and Hancock, W.W. (2013). Mbd2 promotes foxp3 demethylation and T-regulatory-cell function. Mol. Cell. Biol. *33*, 4106–4115.

Watanabe, M., Osada, J., Aratani, Y., Kluckman, K., Reddick, R., Malinow, M.R., and Maeda, N. (1995). Mice deficient in cystathionine beta-synthase: animal models for mild and severe homocyst(e)inemia. Proc. Natl. Acad. Sci. USA *92*, 1585–1589.

Williams, K., Christensen, J., Pedersen, M.T., Johansen, J.V., Cloos, P.A., Rappsilber, J., and Helin, K. (2011). TET1 and hydroxymethylcytosine in transcription and DNA methylation fidelity. Nature *473*, 343–348.

Wu, H., and Zhang, Y. (2014). Reversing DNA methylation: mechanisms, genomics, and biological functions. Cell *156*, 45–68.

Xu, Y., Wu, F., Tan, L., Kong, L., Xiong, L., Deng, J., Barbera, A.J., Zheng, L., Zhang, H., Huang, S., et al. (2011). Genome-wide regulation of 5hmC, 5mC, and gene expression by Tet1 hydroxylase in mouse embryonic stem cells. Mol. Cell *42*, 451–464.

Yamanaka, T., Tosaki, A., Kurosawa, M., Matsumoto, G., Koike, M., Uchiyama, Y., Maity, S.N., Shimogori, T., Hattori, N., and Nukina, N. (2014). NF-Y inactivation causes atypical neurodegeneration characterized by ubiquitin and p62 accumulation and endoplasmic reticulum disorganization. Nat. Commun. *5*, 3354.

Zhang, J., Sio, S.W., Moochhala, S., and Bhatia, M. (2010). Role of hydrogen sulfide in severe burn injury-induced inflammation in mice. Mol. Med. *16*, 417–424.

Zhang, G., Wang, P., Yang, G., Cao, Q., and Wang, R. (2013). The inhibitory role of hydrogen sulfide in airway hyperresponsiveness and inflammation in a mouse model of asthma. Am. J. Pathol. *182*, 1188–1195.

Zheng, Y., Josefowicz, S.Z., Kas, A., Chu, T.T., Gavin, M.A., and Rudensky, A.Y. (2007). Genome-wide analysis of Foxp3 target genes in developing and mature regulatory T cells. Nature *445*, 936–940.

Zheng, Y., Josefowicz, S., Chaudhry, A., Peng, X.P., Forbush, K., and Rudensky, A.Y. (2010). Role of conserved non-coding DNA elements in the Foxp3 gene in regulatory T-cell fate. Nature *463*, 808–812.